ANALYSIS OF BRAIN STEM IN ALZHEIMER MR IMAGES USING REGION BASED LEVEL SET METHOD

A THESIS

Submitted by

SHASHANKA S RAO

EE12B050

in partial fulfillment of the requirements for the degree of

BACHELOR OF TECHNOLOGY (B. TECH)

DEPARTMENT OF ELECTRICAL ENGINEERING

INDIAN INSTITUTE OF TECHNOLOGY MADRAS.

MAY 2016

THESIS CERTIFICATE

This is to certify that the thesis titled **ANALYSIS OF BRAIN STEM IN ALZHEIMER MR IMAGES USING REGION BASED LEVEL SET METHOD**, submitted by Shashanka S Rao, to the Indian Institute of Technology Madras, Chennai for the award of the degree of Bachelor of Technology, is a bona fide record of the research work done by him under our supervision. The contents of this thesis, in full or in parts, have not been submitted to any other Institute or University for the award of any degree or diploma.

Prof. S Ramakrishnan
Research Guide
Professor
Dept. of Applied Mechanics
IIT Madras, 600 036

Prof. Kaushik Mitra
Research Co-Guide
Assistant Professor
Department of Electrical Engineering
IIT Madras, 600 036

Place: Chennai
Date:

ACKNOWLEDGEMENTS

It is my pleasure to thank the people who made this thesis possible by offering their valuable suggestions, constructive criticism, timely help and emotional support.

First and foremost. I would like to thank my supervisor, Dr. S Ramakrishnan for the insightful discussions and continuous support throughout the research period. His guidance helped my understand the problem and motivated me to work hard towards finding the solution to it.

I would like to thank my co-guide, Dr. Kaushik Mitra for all the insights and suggestions regarding the techniques and procedures used as a part of my project. He showed me different ways to approach the problem and helped me remain persistent throughout the project. I would like extend my gratefulness to the Electrical department and Biomedical Engineering department to provide me resources to carry out the project work.

My sincere thanks to all the lab mates, especially Dr. Jack Fredo and Dr. Anandh, K.R who shared their experience and helped me whenever faced with an obstacle. I would also like to thank Mr. Kiran Marri, Mr. Navneeth and Mr. Allmin for all the aid and help provided to envisage this thesis. I would continue to extend my gratitude to all friends in the institute to make my stay in IIT Madras the most memorable event of my life.

Further, I would like to thank my family members who have been a great source of inspiration and strength throughout my life. I am indebted to them for providing me with the opportunities when it mattered the most.

Above all I thank God, for having made everything possible by giving me the strength and courage to do this work.

ABSTRACT

Magnetic resonance imaging (MRI) of the brain anatomical structure uses magnetic fields and radio waves to produce high quality two- or three-dimensional images of brain. Among the different images modes, T1 weighted images are useful for visualizing the anatomy of the brain. Segmentation techniques have been conventionally implemented on these images to extract brain regions such as ventricles, corpus callosum, cerebellum etc. These regions serve as biomarkers for early detection of disorders such as Autism, Alzheimer's, and Parkinson's disease.

Accurate segmentation of brain structures from MR images has been an open challenge mainly due to the absence of clear edges. Recent study on Alzheimer's Disease (AD) have pointed towards brain stem to be the epicenter of the disease but few attempts have been made to decipher the effects of AD on brainstem structures. In this paper, an effort is made to segment brainstem and characterize it as a potential biomarker for detection of AD.

A novel segmentation technique has been proposed to segment brainstem from the mid-sagittal view of the brain. The MR images which were used, are obtained from a public database containing 163 images from AD (CDR = 1) and non-AD (CDR = 0) classes. The MR images used for segmentation were preprocessed using skull-stripping and bilateral filtering. A distance regularized level-set evolution was implemented on the image to segment the brainstem structures. Along with improving the accuracy of segmentation, there has been an added focus on extracting features which could potentially help us classify AD from non-AD MR images. Features such as entropy, area and perimeter were processed using an SVM classifier and validated by a five-fold cross-validation. The brainstem was successfully segmented with an average accuracy of 96% (Pearson's Correlation Coefficient), which is significantly higher than most standard techniques. The mean entropy, area and perimeter of the brainstems extracted from AD MR images were 8.8%, 8.3% and 9.6% lower than brainstems extracted from non-AD MR images, respectively. As this classification can lead to early detection of AD, this work could have clinical significance.

TABLE OF CONTENTS

LIST OF FIGURES

ABBREVIATIONS

AD	Alzheimer's Disease
CSF	Cerebrospinal fluid
MRI	Magnetic resonance imaging
SVM	Support Vector Machine
OASIS	Open Access Series of Imaging Studies
CFL	Classifier Fusion and Labelling
PAM	Profile Active Appearance Model
BAM	Bayesian Appearance Models
EMS	Expectation–maximization-based segmentation
LABS	Landmark-based Automated Brainstem Segmentation
LCC	Largest Connected Component
BET/ BSE	Brain Extraction Tool/ Brain Surface Extractor
LSF	Level Set Function
DRLSE	Distance Regularized Level Set Evolution
PDE	Partial Differential Equation
FPR	False Positive Rate
FNR	False Negative Rate
CDR	Clinical Dementia Rating

CHAPTER 1
INTRODUCTION

Human brain is the primary organ of the human central nervous system. It rests in the head protected by the skull. The adult human brain weighs on an average about 1.3-1.5 kg and roughly occupies a volume of 1130 cm^3 in women and 1260 cm^3 in men (Parent, A et al, 1995). The brain is made up of roughly 100 billion neurons along with glial cells and blood vessels. Some of these neurons (19%) reside in the cerebral cortex and most of the remaining neurons (80%) reside in the cerebellum.

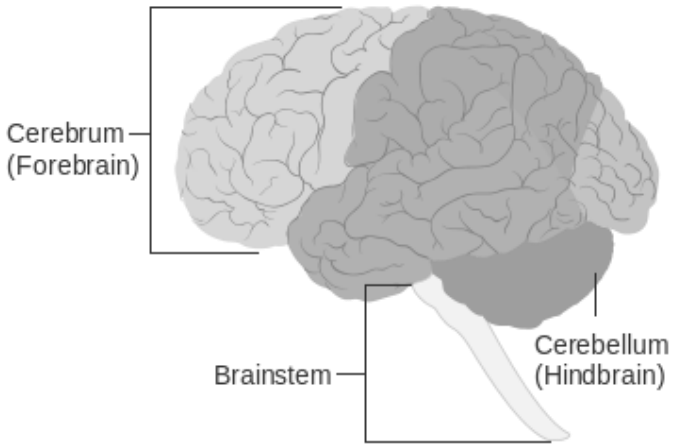

Figure 1.1: A figure of Human brain showing different parts such as cerebrum, cerebellum, brainstem and different lobes

The human brain has many properties that are common to all vertebrate brains, including a basic division into three parts called the forebrain, midbrain, and hindbrain, with interconnected fluid-filled ventricles, and a set of generic vertebrate brain structures including the medulla oblongata and pons of the brainstem, the cerebellum, thalamus, hypothalamus, basal, olfactory bulb etc. (Kristin L. Bigos et al, 2015).

The human brainstem is a complex but highly organized structure, densely packed with long projecting axons and interspersed nuclei. The brainstem is divided into three structures, from superior to inferior: midbrain, pons and medulla oblongata.

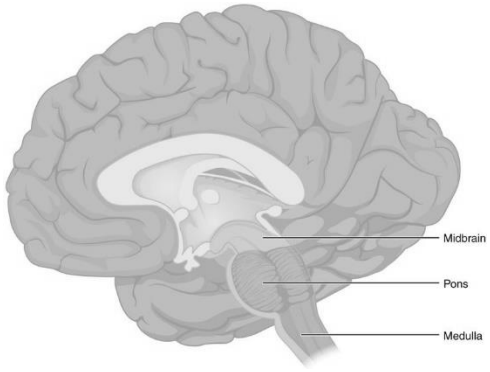

Figure 1.2: A figure of Human brain showing different parts of brainstem such as Medulla, Pons and Midbrain

Each of this structure is responsible for different functions such as: the midbrain is associated with vision, hearing, sleep and motor control, the pons mostly consists of white matter tracts that connect the cerebrum with the medulla. The pons is also connected with the cerebellum through nerve tracts known as the cerebellar peduncles, and contains nuclei associated with functions such as respiration and facial expression. The medulla oblongata connects the rest of the brain to the spinal cord, and regulates cardiac and respiratory functions, as well as reflexes such as swallowing (Juan Eugenio Iglesias et al, 2015). The **mid-sagittal images** gives the maximum area of brain stem and therefore, has been used in this project.

Alzheimer's disease or Alzheimer disease or just AD is responsible for 60-70% of reported dementia. It's a neurodegenerative disorder which is chronic and is generally developed over age. Some of the common symptoms of AD include language problems, memory loss, mood swings and other behavioral issues.

In practice, a diagnosis is largely based on clinical history and examination supported by neuropsychological evidence of the pattern of cognitive impairment (Blennow, K et al, 2010). Researchers are working to uncover as many aspects of Alzheimer's disease and related as possible. Ninety percent of what we know about Alzheimer's has been discovered in the last 15 years. Some of the most remarkable progress has shed light on how Alzheimer's affects the brain. The hope is this better understanding will lead to new treatments. Many potential approaches are currently under investigation worldwide (Kristin L. Bigos et al, 2015).

The identification and validation of biomarkers for diagnosing Alzheimer's disease (AD) and other forms of dementia are increasingly important. To date, ELISA measurement of β-amyloid (1–42), total tau and phospho-tau-181 in cerebrospinal fluid (CSF) is the most advanced and accepted method to diagnose probable AD with high specificity and sensitivity (Christian Humpel, 2011). There has been considerable work on areas of brain such as ventricles with respect to AD. Ventricle enlargement is considered as a significant biomarker in the AD diagnosis.

Brainstem could be a better pathological substrate than any other brain structure due to the fact that AD affects the brainstem first. Simic G et al, in 2009 proved that the symptoms which are prevalent during the early onset of AD, could be traced to the functions of brain stem and connected structures. Although substantial evidence indicates that the progression of pathological changes of the neuronal cytoskeleton is crucial in determining the severity of dementia in Alzheimer's disease (AD), the exact causes and evolution of these changes, the initial site at which they begin, and the neuronal susceptibility levels for their development are poorly understood (Stefan Klöppel et al, 2009).

There is strong evidence from recent studies (Grinberg, L.T et al., 2009 and Simic, G et al, 2009) that early onset of AD could be tracked down to the brainstem, many years before the clinical symptoms are detectable. Despite such importance, the brainstem remains a poorly studied region in brain due to difficulty in segmentation and identification of features.

Level set methods have been consistently used over the past few years to segment brain substructures such as ventricles and corpus callosum. Chunming Li, et al, in 2010, proposed a Distance-regularized level set method which could evolve the level set contour without any hassle regarding re-initialization. This technique has been extensively used in this thesis to segment the brainstem structures successfully. The segmentation was then verified for accuracy using indices and coefficients such as Dice and Jaccard. Such comparative measures are then compared with standard segmentation techniques which are discussed in detail in the literature section.

Before any technique is implemented on an image, it is essential to have excellent preprocessing techniques to speed up the algorithms used. Bilateral filtering along skull-stripping has been proposed in this thesis. Skull-stripping has been carried to remove noise due to presence of skull of CSF protecting the brain. Also, all the features which are to be used in the process of classification need to be normalized with respect to brain size, which wouldn't be possible without skull-stripping. Bilateral filter is an edge-preserving filter which enhances the edge but also smoothens the image.

There has been recent interest in machine learning techniques such as support vector machines (SVMs) to categorize individual structural or functional brain images by differentiation of images from two groups (e.g. male/female or patient/control). Therefore, an attempt has been made to classify the AD and non-AD classes using SVM after extracting some features from brain stem. As the results are not very promising with respect to these machine learning techniques, average statistics have also been noted down in the results section. (Stefan Klöppe et al, 2008).

Inspired by recent work on gender differences in the occurrence of Alzheimer's disease (Musicco M. et al, 2009), some statistics have also been drawn on effect of gender variation on AD-affected brainstem. Prevalence studies on dementia generally show a higher risk in women than in men. The dataset taken from OASIS is skewed in terms of gender of the patients with AD (nearly two times as many females as males). But the impact of AD on brainstem is more severe in terms of males than females which is verified by literature.

.

CHAPTER 2
LITERATURE REVIEW

In this section we would discuss the different methods which are being used to segment brainstem structures from MRI. Most of these techniques are very relatively new given the fact that brainstem has been identified as a biomarker to identify diseases such as AD, only recently. Some of the conventional techniques have been discussed first, followed by more hybrid techniques. The conventional techniques are very prominent and wide-spread as they are more general and can be implemented to segment most of the brain structures.

2.1. Classifier Fusion and Labelling (CFL)

This technique was first proposed by P. Aljabar et al, in 2007. It is possible to obtain a structural segmentation by propagating labels from multiple atlases to the query subject, treating them as classifiers and fusing them to achieve a consensus estimate. This approach can be viewed as an extension of atlas-based segmentation methods. Classifier fusion, based on the majority vote rule, has been shown to be robust and accurate when used to segment brain structures.

However, problems of scale occur when classifier fusion is used in conjunction with a large repository of labelled atlases. These problems are discussed in Aljabar et al. (2007) and schemes for the selection of smaller numbers of appropriate classifiers, prior to propagation and fusion, are presented.

2.2. Profile Active Appearance Model (PAM)

Dimitris Metaxas et al, in 2008 proposed a novel algorithm called Active Appearance Model (AAM) is a statistical model of both the shape of a structure and its appearance,

together with an algorithm for matching it to an image. The method described here uses a variant of AAMs which models the intensities along profiles that are normal to the boundary of a structure. During image search the model is capable of synthesizing the texture across the surface of the object of interest, and the residual differences between the synthesized texture and that in the query image are used to drive the search.

Separate models have to be constructed for each of the several structures, and a composite model containing all structures is also constructed. In this two layer approach the composite model has a lower degree of freedom than the single structure models and its search results are less accurate. However, the composite model is less prone to falling into local minima, and its results are used to provide good initialization for the single structure models which give more accurate results.

2.3. Bayesian Appearance Models (BAM)

Similar to the profile AAM, the BAM models texture along the normal to a surface representation of the structural boundary. Joan Alabort-i-Medina et al in 2014 published their work on BAM. The BAM also restricts the search space to linear combinations of the eigenvectors of a shape model. The BAM differs mainly in the method of representing the relationship between shape and intensity which is modelled via the conditional distribution of intensity given shape. Rather than synthesizing a single predicted intensity image, the predicted intensity distribution is calculated. This is the conditional distribution of intensity given the shape (vertex locations). The BAM aims to maximize the probability of the shape given the observed intensities.

2.4. Expectation–maximization-based segmentation using a brain atlas (EMS)

K Van Leemput et al, in 2003 proposed a probabilistic approach to brain segmentation, combining a standard expectation–maximization with a brain atlas constructed from the

training data. Such a technique require a lot of training data which hasn't been utilized in this thesis.

In structures with more subject-specific individual and elongated shapes or shape pose, such as brain stem and associated fourth ventricles, registration errors in the atlas construction and mapping phase can propagate to the final EM classification.

The following techniques are more hybrid techniques which have seen the light over the past couple of years. These techniques are specific to brainstem segmentation and have high degrees of accuracy.

2.5. Bayesian segmentation of brainstem structures in MRI

Juan Eugenio Iglesias et al, in their paper in 2015 discuss the various Bayesian methods to segment brainstem structures. The segmentation method relies on a probabilistic atlas of the brainstem and its neighboring brain structures. To build the atlas, they combined a dataset of 39 scans with already existing manual delineations of the whole brainstem and a dataset of 10 scans in which the brainstem structures were manually labeled with a protocol that was specifically designed for this study. The resulting atlas can be used in a Bayesian framework to segment the brainstem structures in novel scans. The segmentation method is robust to changes in MRI contrast or acquisition hardware. The results show that, when used simultaneously, the volumes of the midbrain, pons and medulla are significantly more predictive of age than the volume of the entire brainstem, estimated as their sum. The results also demonstrate that the method can detect atrophy patterns in the brainstem structures that have been previously described in the literature. The proposed algorithm is also able to detect differential effects of AD on the brainstem structures.

Because the appearance of the brainstem is relatively flat in the MRI scans of all the datasets used in this study, a single Gaussian was found to suffice to model the intensities within each tissue type. Since no ground truth was available for their dataset, the robustness was assessed by visually inspecting the outputs and grading each segmentation as satisfactory or unsatisfactory.

2.6. Multiparametric brainstem segmentation using a modified multivariate mixture of Gaussians

A modified multivariate mixture of Gaussians (mmMoG) was applied to the problem of multichannel tissue segmentation. By using quantitative magnetization transfer and proton density maps acquired at 3 T with 0.8 mm isotropic resolution, tissue probability maps for four distinct tissue classes within the human brainstem were created.

$$p\left(x_{ij}\middle|\mu_k.S_k\right) = \frac{1}{\sqrt{(2\pi)^M \det|S_k|}} \exp\left(-\frac{1}{2}\left(x_{ij}-\mu_k\right){S_k}^{-1}\left(x_{ij}-\mu_k\right)\right) \qquad (Eq\ 2.1)$$

It was the first method to allow accurate automated segmentation of the human brainstem in vivo. By developing a multimodal segmentation algorithm using mmMoG, brainstem specific tissue probability maps could be generated for four distinct brainstem tissue classes. These probability maps could then be utilized within the pre-existing SPM framework to allow individual segmentation of the brainstem in vivo (Christian Lambert et al, 2013)

2.7. Landmark-based Automated Brainstem Segmentation (LABS)

LABS processes high-resolution structural magnetic resonance images (MRIs) according to a revised landmark-based approach integrated with a thresholding method, without manual interaction. This method was first tested on morphological T1-weighted MRIs of 30 healthy subjects. Its reliability was further confirmed by including neurological patients (with Alzheimer's disease) from the ADNI repository, in whom the presence of volumetric loss within the brainstem had been previously described. Landmarks for the brainstem structures were derived from first segmenting other structures such as corpus callosum. This method of the least accurate method amongst all as identifying landmarks is very erroneous. (Salvatore Nigro et al, 2014)

CHAPTER 3

METHODOLOGY: SEGMENTATION OF BRAINSTEM STRUCTURES USING LEVEL SET METHOD

The methodology used in segmentation and analysis of the Brainstem is as follows:

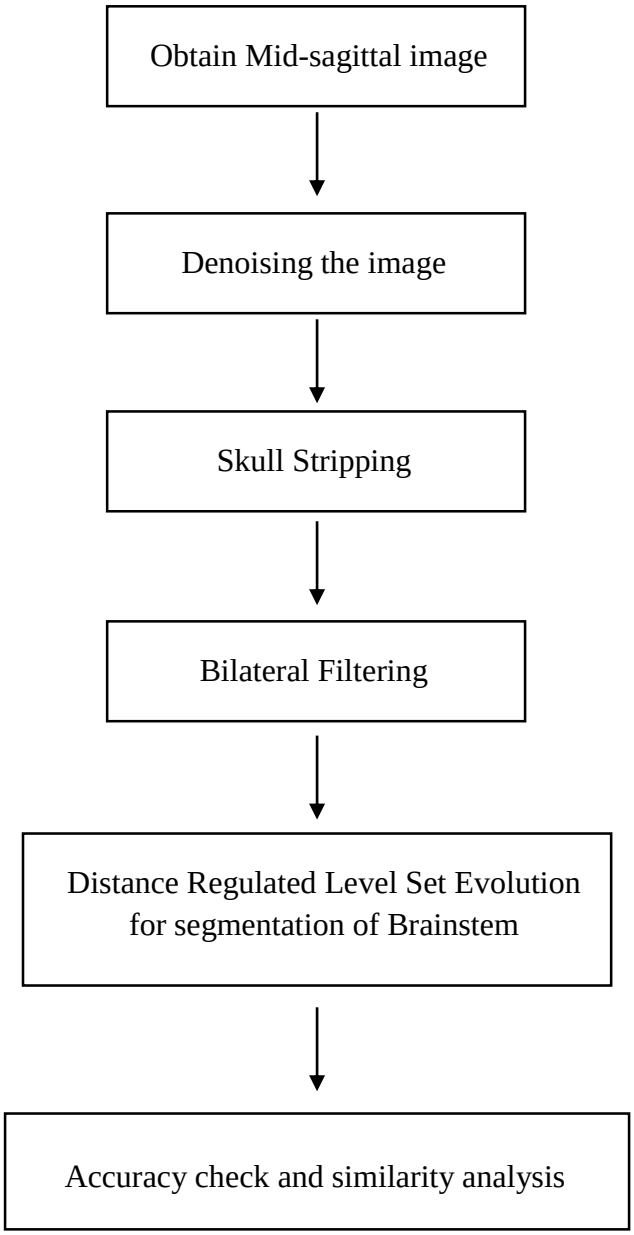

The first two sections in this chapter discusses the literature review for pre-processing techniques involved in my segmentation procedures. These are skull-stripping and bilateral filtering namely. Such pre-processing techniques are required for denoising (Gaussian Kernel) and cleaning the images for faster and accurate implementation of subsequent algorithms.

1.1. Skull Stripping

Skull stripping methods are designed to eliminate the non-brain tissue in magnetic resonance (MR) brain images. Removal of non-brain tissues is a fundamental step in enabling the processing of brain MR images. Three-dimensional brain images have become increasingly popular in medical applications. These images are being used for research, diagnosis, treatment, surgical planning, and image guided surgeries. However, several pre-processing methods are required before these images can be employed, such as image segmentation (Chunming Li, 2010), image registration (Klein et al., 2010), inhomogeneity correction (Wels et al., 2011) and many more techniques involving the human brain. Many of these methods achieve a brain extraction using a skull stripping process as first step, to eliminate non-brain tissue present in the image. Therefore, it is imperative to have accurate skull stripping methods available to avoid time consuming manual corrections that are not systematic and cannot be applied routinely.

Magnetic Resonance Images (MRI) are used to analyze the human organs without surgery. Brain image segmentation is one of the most important tools and hence need by the clinicians. However, an accurate segmentation is a significant task and crucial for exact diagnosis. K.Somasundaram et al, have proposed automated method for segmenting brain from T1 weighted MR images. Initially, Otsu thresholding technique is used to find the threshold value in order to eliminate low intensity pixels such as air and CSF from the image. K-Mean clustering technique is used to classify the image into three parts such as brain tissues, non-brain tissues and background. To eliminate non-brain pixels, we have analyzed histogram of the image and finally Largest Connected Component (LCC) is used to segment the brain (K.Somasundaram, 2014)

Andre G.R Balan et al, in paper discuss a smart histogram analysis applied to this skull-stripping problem in T1-weighted MRI. This paper differs from the Somasundaram's paper in a manner where a Binary Mathematical Morphology is used before the final Brain Mask. Otsu thresholding is the commonly followed thresholding algorithm (Andre G.R Balan et al, 2012). In addition, the reliability of these processes is essential because any error at this first step will be difficult to correct in subsequent processing steps.

Some of most common skull-stripping toolboxes used are brain extraction tool (BET) and brain surface extractor (BSE). The above papers have developed algorithms which perform much better than these algorithms. The Jaccard coefficients for skull-stripping technique used in this project is close to 0.97 whereas BSE and BET do not perform better than 0.76 and 0.89 on an average (K.Somasundaram, 2014)

1.2. Bilateral filtering

The bilateral filter is a non-linear technique that can blur an image while respecting strong edges. Its ability to decompose an image into different scales without causing haloes after modification has made it ubiquitous in computational photography applications such as tone mapping, style transfer, relighting, and denoising. Sylvain Paris et al, 2008 work on this filtering technique provides a graphical, intuitive introduction to bilateral filtering, a practical guide for efficient implementation and an overview of its numerous applications, as well as mathematical analysis.

The intensity value at each pixel in an image is replaced by a weighted average of intensity values from nearby pixels. This weight can be based on a Gaussian distribution. Crucially, the weights depend not only on Euclidean distance of pixels, but also on the radiometric differences (e.g. range differences, such as color intensity, depth distance, etc.). This preserves sharp edges by systematically looping through each pixel and adjusting weights to the adjacent pixels accordingly.

The equations for such a filter are as follows,

$$BF[I]_p = \frac{1}{W_p} \sum_{q \in S} G_{\sigma_s}(\|p - q\|)\, G_{\sigma_r}(|I_p - I_q|)\, I_q \qquad (Eq\ 3.1)$$

Where normalization factor W_p ensures pixel weights sum to 1.0

$$W_p = \sum_{q \in S} G_{\sigma_s}(\|p - q\|)\, G_{\sigma_r}(|I_p - I_q|) \qquad (Eq\ 3.2)$$

Parameters σ_s and σ_s will specify the amount of filtering for the image I. G_{σ_s} is a spatial Gaussian weighting that decreases the influence of distant pixels, G_{σ_r} is a range Gaussian that decreases the influence of pixels q when their intensity values differ from I_p.

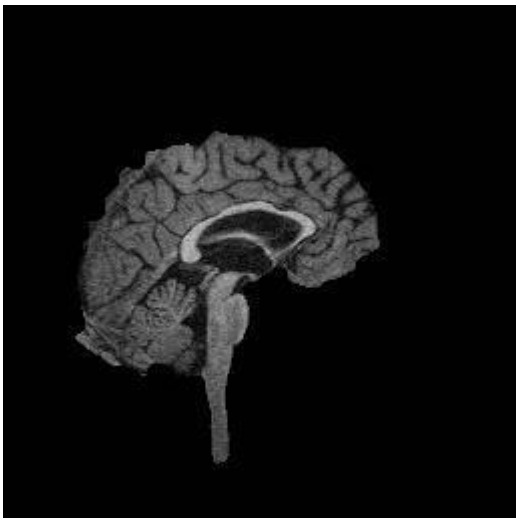

Figure 3.1: A representative MR image after skull stripping

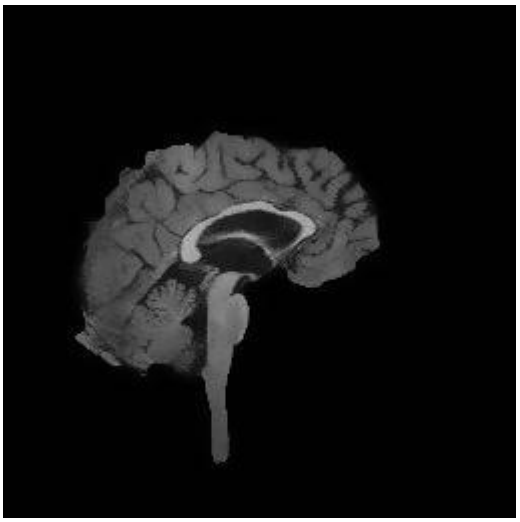

Figure 3.2: A representative skull-stripped MR image after bilateral filtering

We see from the above images that, due to bilateral filtering, the edges have been preserved whereas the image has been smoothened overall. Such filtering techniques are very useful as the level set evolution becomes faster.

1.3. Distance Regularized Level Set Evolution

Level set methods have been widely used in image processing and computer vision. In conventional level set formulations, the level set function typically develops irregularities during its evolution, which may cause numerical errors and eventually destroy the stability of the evolution. Therefore, a numerical remedy, called initialization, is typically applied to periodically replace the degraded level set function with a signed distance function.

The level set evolution is derived as the gradient flow that minimizes an energy functional with a distance regularization term and an external energy that drives the motion of the zero level set toward desired locations.

$$\frac{\partial C(s,t)}{\partial t} = FN \qquad (Eq\ 3.3)$$

Where F is the speed function that controls the motion of the contour and N is the inward normal vector to the curve C. The above equation can be converted by replacing the dynamic contour $C(s,t)$ as the zero level set of a time dependent LSF $\phi(x,y,t)$. Assuming that the embedding LSF ϕ takes negative values inside the zero level contour and positive values outside, the inward normal vector can be expressed as $N = -\nabla\phi/|\nabla\phi|$, where ∇ is the gradient operator.

$$\frac{\partial \phi}{\partial t} = F|\nabla\phi| \qquad (Eq\ 3.4)$$

The distance regularization effect eliminates the need for initialization and thereby avoids its induced numerical errors. In contrast to complicated implementations of conventional level set formulations, a simpler and more efficient finite difference scheme can be used to implement the DRLSE formulation.

When the distance regularized term is added to the PDE, it becomes

$$\frac{\partial \phi}{\partial t} = \mu\, div\big(d_p|\nabla\phi|\big)|\nabla\phi| + F|\nabla\phi| + A.\nabla\phi \qquad (Eq\ 3.5)$$

With distance regularization term, numerical scheme is stable without the need for re-initialization. DRLSE can be used for image segmentation including region-based or edge-based image formation to define the external energy.

In level set methods, a contour (or more generally a hypersurface) of interest is embedded as the zero level set of an LSF. Although the final result of a level set method is the zero level set of the Level Set Function (LSF), it is necessary to maintain the LSF in a good condition, so that the level set evolution is stable and the numerical computation is accurate. This requires that the LSF is smooth and not too steep or too flat (at least in a vicinity of its zero level set) during the level set evolution (Chunming Li, 2010)

The energy equation corresponding to the energy function $\varepsilon(\phi)$,

$$\varepsilon(\phi) = \mu\mathcal{R}_p + \lambda\mathcal{L}_g + \alpha A_g(\phi) \qquad (Eq\ 3.6)$$

where $\mathcal{R}_p$ is level set regularization, $\lambda > 0$ and $\alpha\, \epsilon\, R$ are coefficients of the energy functional $\mathcal{L}_g(\phi)\ and\ A_g(\phi)$

$$\mathcal{R}_p = \int p(|\nabla\phi|dx \qquad (Eq\ 3.7)$$

$$\mathcal{L}_g(\phi) = \int g\delta(\phi)(|\nabla\phi)\, dx \qquad (Eq\ 3.8)$$

$$A_g(\phi) = \int gH(-\phi)\, dx, \quad where\ g \triangleq \frac{1}{1 + |\nabla G_\sigma * I|^2} \qquad (Eq\ 3.9)$$

A_g is speed of level set function accelerated and $\mathcal{L}_g$ is minimum when the level set function is at object boundary. p is the potential (double walled in the case of region based) and G_σ is a Gaussian Kernel with a standard deviation σ.

3.3.1 Initialize the level set function

$Coefficient\ of\ the\ weighted\ length\ term\ L\ (\lambda) = 5$

$Coefficient\ of\ the\ weighted\ area\ term\ A\ (\alpha) = -2.5$

$Coefficient\ of\ the\ distance\ regularization\ term\ R\ (\mu) = 0.2$

$Parameter\ that\ specifies\ the\ width\ of\ the\ Dirac\ Delta\ function\ (\epsilon) = 1.5$

Alpha (α) is an important parameter which governs the evolution of the level set. More negative the value of α, lesser is the sensitivity in edge detection. By trial and error, it was estimated that for the above given parameters, 500 iterations of the level set evolution segments the brainstem successfully.

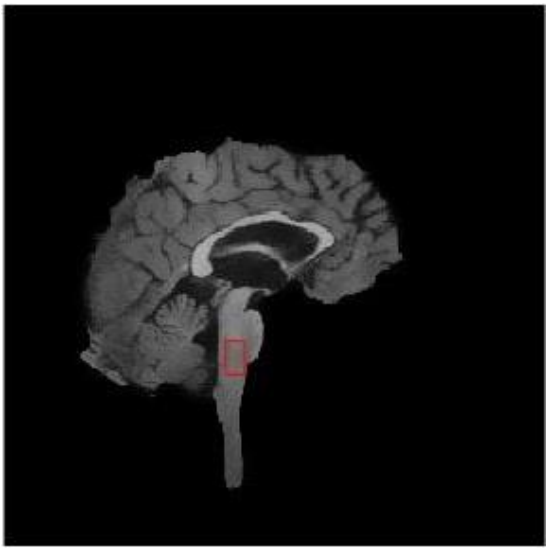

Figure 3.3: Drawing a rectangular box on the MR image to mark the initial level set contour

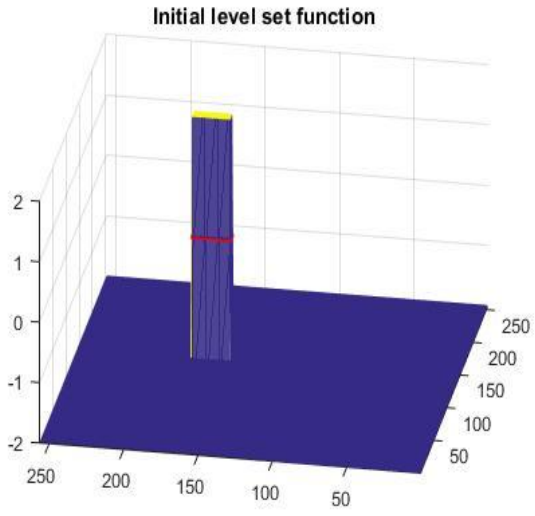

Figure 3.4: Visualization of the initial contour on a 3D potential diagram

3.3.2 Evolution of level set function to form the final contour

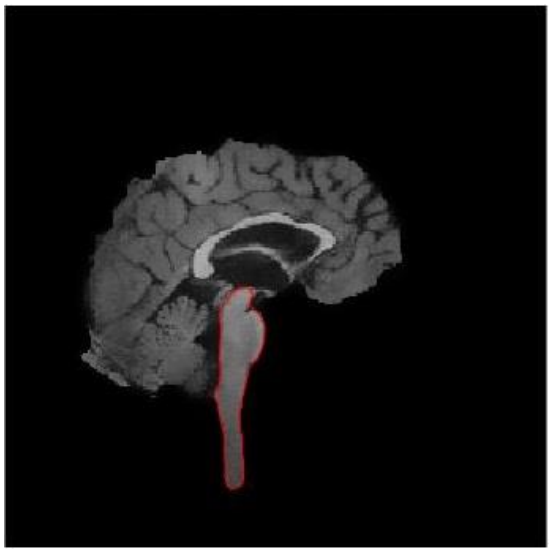

Figure 3.5: The final evolved contour after multiple iterations

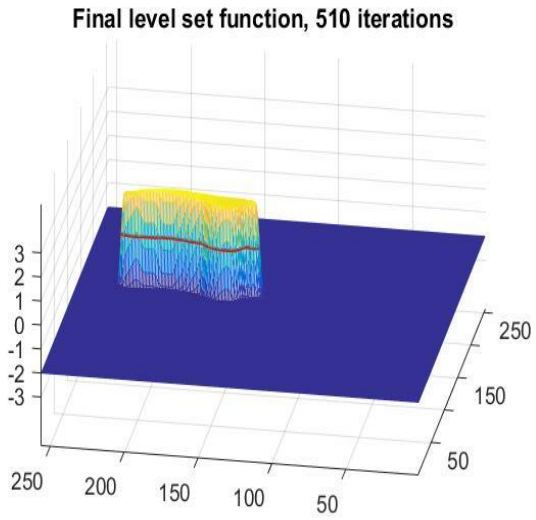

Figure 3.6: Visualization of the final contour on a 3D potential diagram

1.4. Analysis of segmented Brainstem structures

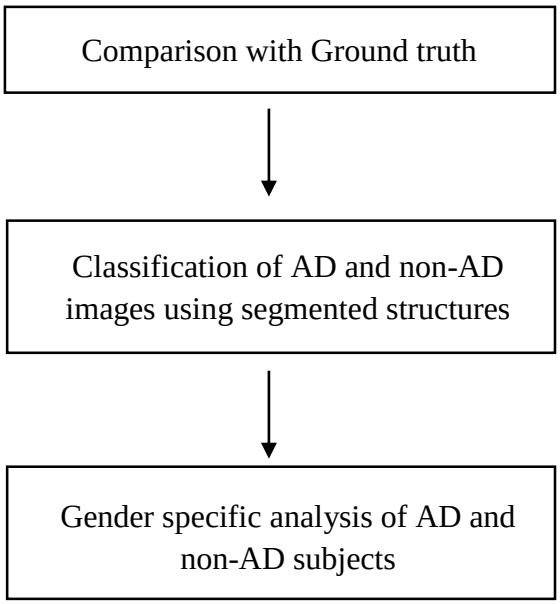

3.4.1 Comparison with Ground truth

For the sake of comparison with ground truth images, certain coefficients such as Jaccard and Dice are used. Overlap ratio measures are a compromise that applies to many situations. Unlike volume error, they are sensitive to misplacement of the segmentation label, but they are relatively insensitive to volumetric under- and overestimations. Shape infidelity is only captured if the deviation is volumetrically impactful: a thin panhandle won't result in a large deviation from one. The Dice similarity index is currently more popular than the Jaccard overlap ratio. This is unfortunate because Jaccard is numerically more sensitive to mismatch when there is reasonably strong overlap. A drawback of both is that they are unsuitable for comparing segmentation accuracy on objects that differ in size (Rohlfing et al. 2004). False Positive Rate (FPR) is used to measure the degree of over-segmentation and False Negative Rate (FNR) is a measure of under-segmentation.

$$Dice\ Coefficient\ = \frac{2|X\ \cap Y\ |}{|X| + |Y|} \qquad (Eq\ 3.10)$$

$$Jaccard\ Index\ or\ Coefficient\ = \frac{|X\ \cap Y|}{|X\ \cup Y|} \qquad (Eq\ 3.11)$$

$$False\ Positive\ Rate = \frac{|X\ \cap Y^c|}{|X\ \cup Y|} \qquad (Eq\ 3.12)$$

$$False\ Negative\ Rate = \frac{|X^c \cap\ Y\ |}{|X\ \cup Y|} \qquad (Eq\ 3.13)$$

$where\ |X|\ and\ |Y|\ are\ segmented\ and\ ground\ truth\ images\ respectively$

The ideal values for Dice and Jaccard are 1 and FPR and FNR have an ideal value of 0. The average values of these values are taken for segmented images and also compared with existing techniques.

3.4.2 Classification and comparison of AD and non-AD images

The data from OASIS contains nearly twenty seven AD images with CDR (Clinical Dementia Rating) =1. Another twenty nine non-AD images, i.e. with CDR = 0 have been considered in the pursuit of finding features to classify AD from non-AD using brainstem as a biomarker.

SVM was used to classify the two sets of images with area ratio, perimeter ratio and entropy as the three features. A K-fold SVM was used to classify these images. Apart from all these machine learning techniques, average statistics were also used as the data samples are not large enough.

Based on the paper by Vina J et al, 2010, it has been found that the Alzheimer's disease can also be gender selective. Some statistics are also drawn on this behalf to compare and contrast between brainstem images of AD and non-AD patients among male and females separately.

Some of the features which are used for this classification are as follows:

- Entropy is a statistical measure of randomness that can be used to characterize the texture of the input image (**This can measure changes in white and gray matter content in brain structures)**

$$Entropy = -\sum p\ log_2 p\ , p\ is\ the\ histogram\ counts\ of\ the\ image \qquad (Eq\ 3.14)$$

- Area/perimeter ratio measures the quotient of area/perimeter of segmented brain stem in its mid-sagittal view to the mid-sagittal image of its skull-stripped brain

$$AR\ or\ PR = \frac{Area/perimeter\ of\ brain\ stem}{Area/perimeter\ of\ brain\ (skull - stripped)} \qquad (Eq\ 3.15)$$

RESULTS AND DISCUSSIONS

2.1. Visual inspection of MR images

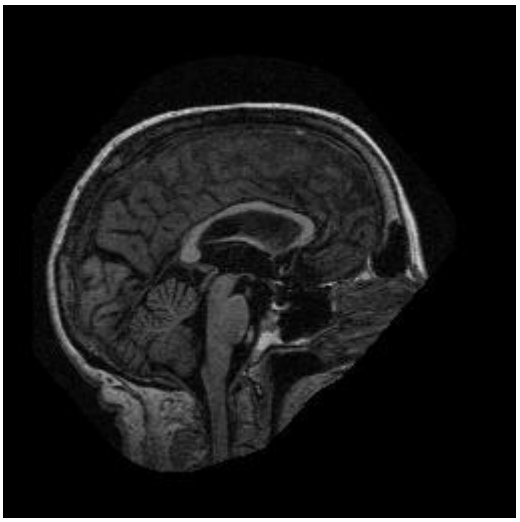

Figure 4.1: A representative MR image of a non-AD subject (CDR = 0)

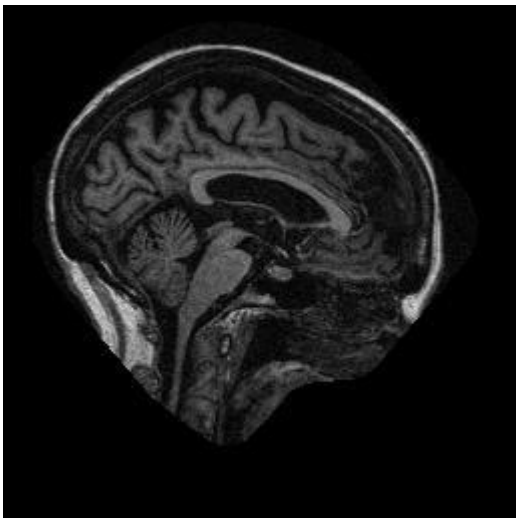

Figure 4.2: A representative MR image of an AD subject (CDR = 1)

By visual inspection we can see some fundamental differences in the two images above. We see that there is an atrophy in regions of brain such as corpus callosum and brain stem. During Alzheimer's, there is an enlargement of ventricular regions of brain leading to pressure exerted on structures such as corpus callosum and brain stem leading to their shrinkage. A major contributor to the atrophy of such structures is due to the neuronal degradation in these areas.

There is also a noticeable difference in the texture of the brain MR images of AD and non-AD subjects. These differences suggest that some features such as area of brain stem in the mid-sagittal plane can be used successfully to classify AD from non-AD test subjects. As there is a difference in texture, simple parameters such as entropy of the image can be used to differentiate these images.

2.2. Results of Skull-stripping

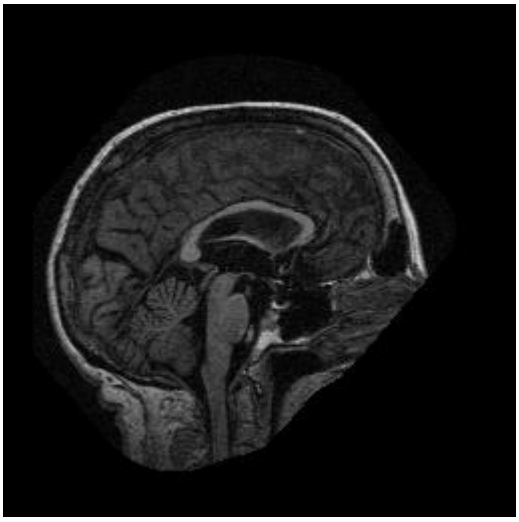

Figure 4.3: A representative noisy MR image of a non-AD test subject

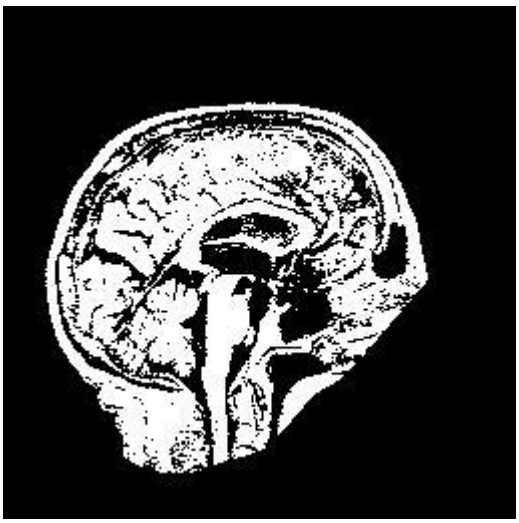

Figure 4.4: A representative MR image after denoising and Otsu Thresholding

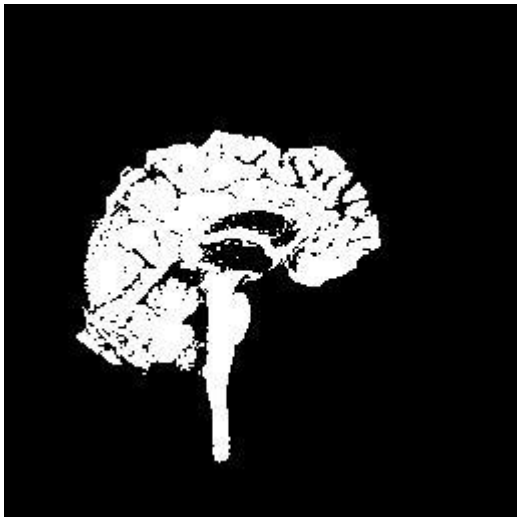

Figure 4.5: A representative image, after K-means clustering and LCC, which can be used as binary mask

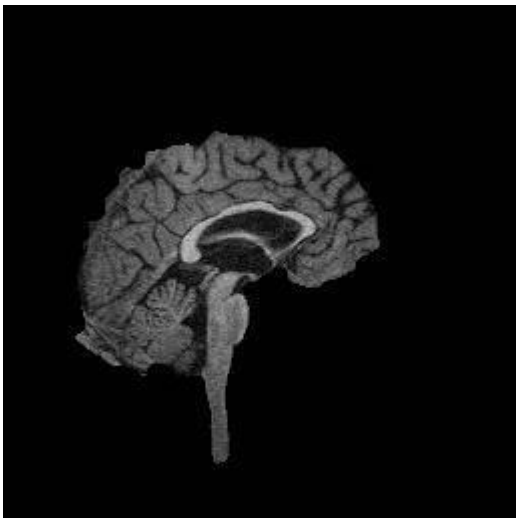

Figure 4.6: A representative skull stripped image after the binary mask is used on the original image

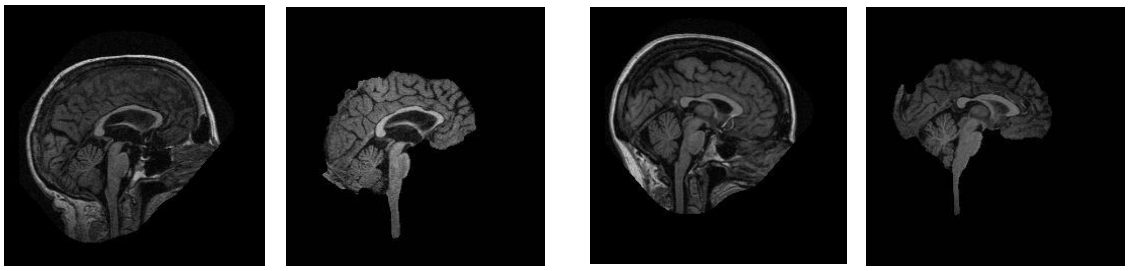

Figure 4.7: The above images are examples of skull-stripping for non-AD MR images

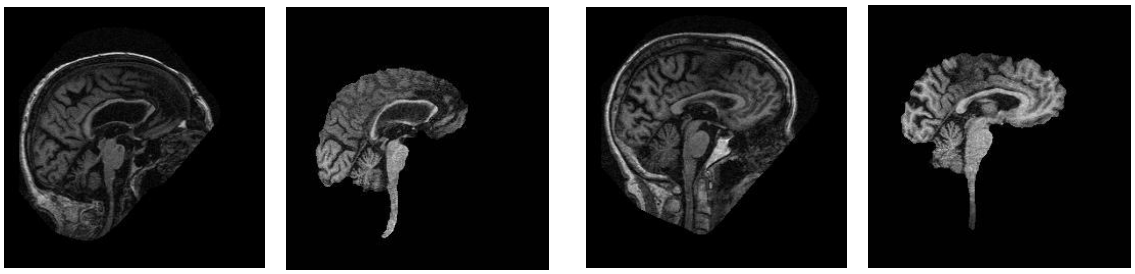

Figure 4.8: The above images are examples of skull-stripping for AD MR brain images

2.3. Results of Level Set Evolution

Figure 4.9: Sequence of brain stem segmentation for a representative MR image for non-AD (top row) and AD (bottom row) test subject.

2.4. Accuracy analysis of segmentation

Measure	Ground Truth value	Obtained Values
Jaccard Index	1	0.9196
Dice Coefficient	1	0.9467
FPR (Over segmentation)	0	0.0899
FNR (Under segmentation)	0	0.0210

Table 4.1: The above table compares the experimental values with ideal ground truth values

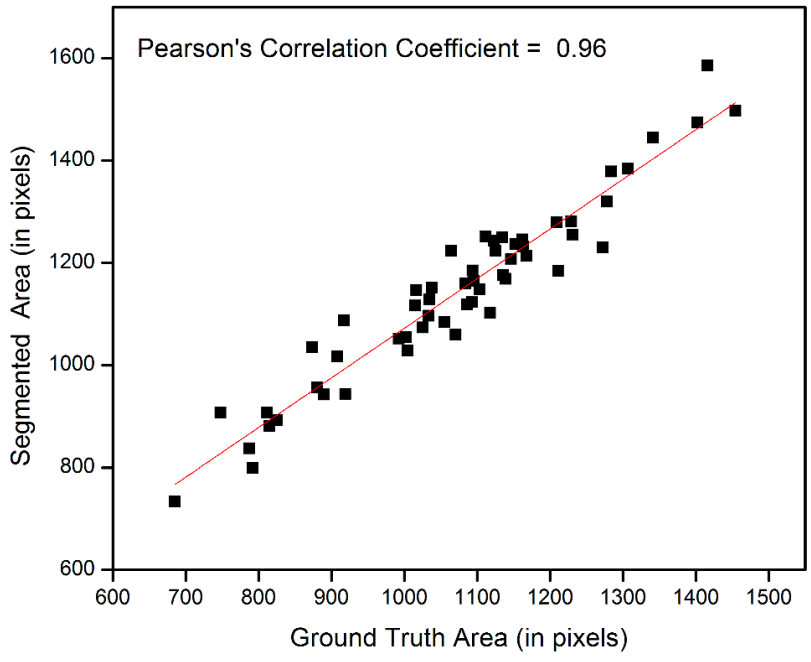

Figure 4.10: Scatter plot between areas of ground truth and segmented images using Distance regularized level set evolution method

4.4.1 Comparison of segmentation technique for MR images with standard techniques

The below comparisons are taken from Kolawole Oluwole Babalola et al, paper in 2009. He compared and contrasted four different techniques (CFL, PAM, BAM and EMS) to segment the brain stem.

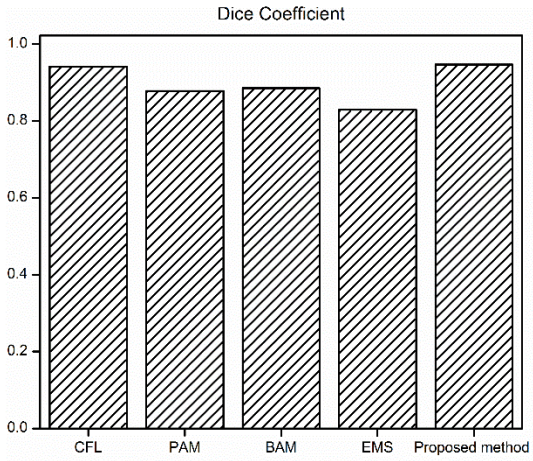

Figure 4.11: A bar graph comparing Dice Coefficients of different segmentation techniques

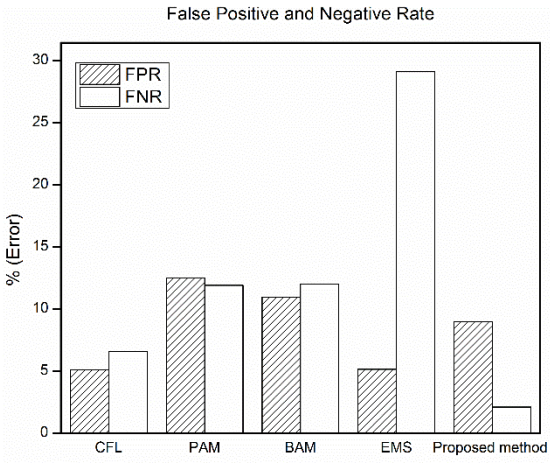

Figure 4.12: A bar graph comparing FPR and NPR of different segmentation techniques

We see that the proposed technique outperforms the existent standard techniques in Dice Coefficients and False Negative Rates. False Positive rates are at par with the best technique (CFL). The coefficients and indices were calculated for 56 MR images (27 AD and 29 non-AD).

4.4.2 Comparison of segmentation technique for AD and non-AD MR images

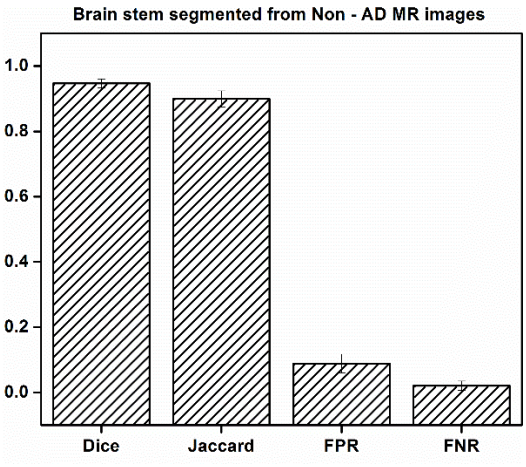

Figure 4.13: A bar graph showing accuracy measures for Non-AD MR images

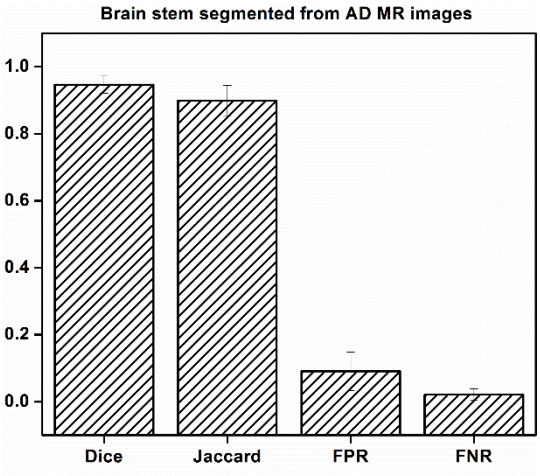

Figure 4.14: A bar graph showing accuracy measures for AD MR images

We can observe that the coefficients are not very different for both the sets of images. Only the standard deviation seems to be noticeably higher for AD images owing to some images being very noisy.

2.5. Classification of AD and non-AD classes using brain stem as a biomarker

The features which have been extracted to classify the AD and non-AD MR images are:

- Area ratio of mid-sagittal brain stem
- Perimeter ratio of mid-sagittal brain stem
- Entropy of the image of mid-sagittal brain stem

4.5.1 Average and mean statistics

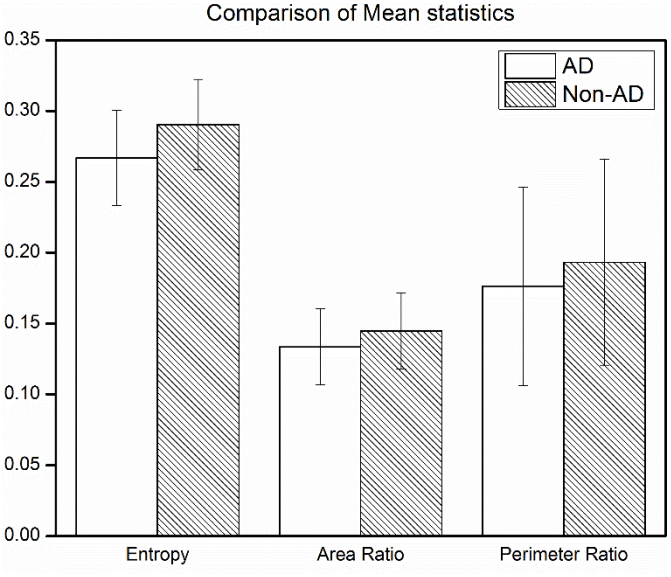

Figure 4.15: A bar graph comparing mean statistics of brain stems extracted from AD and non-AD test subjects

We see that the Non-AD image have an offset with respect to all the 3 features considered. The entropy (randomness of texture) of the segmented brain stems from AD MR images are 8.8% higher than the ones from non-AD MR images. The area ratio (area of brain stem in mid-sagittal section to skull-stripped brain) and the perimeter ratio (perimeter of brainstem in mid-sagittal section to skull-stripped brain) for non-AD brain stems are 8.3% and 9.6% higher than AD affected brain stems, respectively.

4.5.2 Classification using k-fold SVM

For performing k-fold SVM, 20 images out of 56 were randomly selected as test data and the rest were used for training the SVM model. The two classes used for classification were AD and non-AD. The features used for classification were entropy and mid-sagittal area of brain stem. A 4-fold classification is used as the number of the data points are few.

Here are the results of the 4-Fold (Cross-validation) SVM classification:

Accuracy ($\frac{TP+FN}{TP+NP+TN+FP}$)	Specificity ($\frac{TN}{FP+TN}$)	Precision ($\frac{TP}{TP+FN}$)
0.625	0.600	0.690

Table 4.2: The above table displays the results of the SVM classification

We see that the accuracy of this classification is 62.5%. The accuracy is reduced to some images in AD class which haven't shown any brain stem shrinkage. Other features such as ventricular expansion or atrophy of corpus callosum has be to be engaged to improve these results.

4.6 Effect of gender type on brain stem features for AD patients

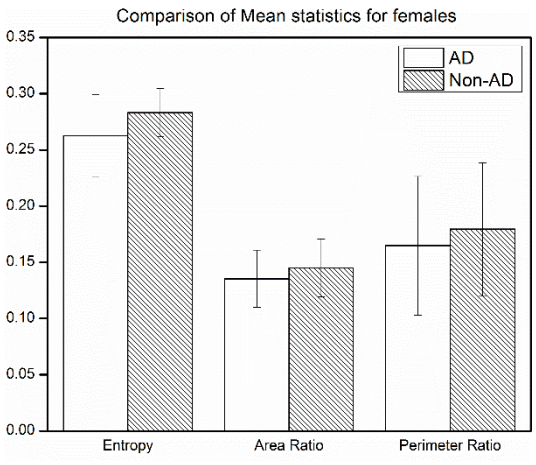

Figure 4.16: A bar graph comparing mean statistics of brain stems extracted from female AD and non-AD test subjects

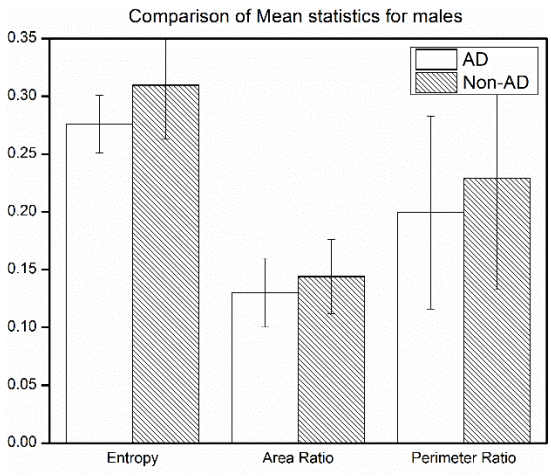

Figure 4.17: A bar graph comparing mean statistics of brain stems extracted from male AD and non-AD test subjects

Gender	Feature	Percentage difference between AD and non-AD MR brain stem images
Male	Entropy	12.3 %
	Area Ratio	10.7 %
	Perimeter Ratio	14.8 %
Female	Entropy	7.8 %
	Area Ratio	7.17 %
	Perimeter Ratio	8.9 %

Table 4.3: The above table presents the percentage change in feature values between AD and non-AD MR images for both the genders separately

We see that the effect on the Alzheimer's disease is slightly more prominent on males than females with respect to brain stem features.

4.7 Discussion

The segmentation technique is highly efficient with Pearson's correlation index of 96% and low NPR and FPR. We see that the proposed technique outperforms the existent standard techniques in Dice Coefficients and False Negative Rates. False Positive rates are at par with the best technique (CFL).

The segmentation accuracies are nearly identical for both AD and non-AD MR images expect for varying standard deviations in values of different indexes. This can be attributed to some AD MR images being very noisy.

The entropy is higher for non-AD images in comparison to AD images. This is due to change in grey matter and white matter content due to the effect of AD on brainstem. The area and perimeter of the AD images have been reduced due to possible atrophy of the brain stem which is a common feature of AD affected brain tissues (Blennow, K et al, 2010).

The cross-validation don't produce very promising results as there are a significant number of images in AD class which do exhibit any atrophy. We would need to consider other features to improve the accuracy of classification. We also observe minor differences in difference in such features in males and females, which has can also be verified from literature (Musicco M, et al, 2009)

4.8 Future Scope

A major area which could be explored is the internal segmentation of brain stem into Pons, Midbrain and Medulla Oblongata. This segmentation could shed light into how individual substructures are affected by AD. Furthermore, more features could be extracted and the classification can be made more extensive and accurate.

Age related study could be carried out along with gender related study. AD rarely affects people below the age of 50 but such rare cases can be of great clinical significance. As it is very hard to distinguish age-related dementia and AD, research on AD in young individuals will definitely help us identify unique features which could help us analysis and classify AD.

The segmentation technique can be improved by more pre-processing techniques such as particle filtering and features such as wavelet entropy index can achieve higher accuracy in classification.

REFERENCES

1. Parent, A; Carpenter MB (1995). "Ch. 1". Carpenter's Human Neuroanatomy. Williams & Wilkins. ISBN 978-0-683-06752-1.

2. Kristin L. Bigos, Ahmad R. Hariri, Daniel R. Weinberger (2015). “Neuroimaging Genetics: Principles and Practices”. Oxford University Press. p. 157. ISBN 0199920222. Retrieved January 2, 2016.

3. Juan Eugenio Iglesias, et al. “Bayesian segmentation of brainstem structures in MRI”, NeuroImage 113 (2015) 184–195

4. Blennow, K., et al. “Biomarkers in Alzheimer's disease drug development”. Nature Medicine 16, 1218–1222 (2010)

5. Grinberg, L.T., et al., 2009. “The dorsal raphe nucleus shows phospho-tau neurofibrillary changes before the transentorhinal region in Alzheimer's disease. A precocious onset?” Neuropathology and Applied Neurobiology 35 (4), 406–416.

6. Simic, G., Stanic, G., Mladinov, M., Jovanov-Milosevic, N., Kostovic, I., Hof, P.R., 2009. “Does Alzheimer's disease begin in the brainstem?” Neuropathology and Applied Neurobiology 35 (6), 532–554.

7. Stefan Klöppel , et al. “Automatic classification of MR scans in Alzheimer's disease” Brain: A Journal of Neurology, Volume 131, Issue 3 Pp. 681 - 689

8. Andre G.R. Balan, et al. “Smart histogram analysis applied to the skull-stripping problem in T1-weighted MRI”, Computers in Biology and Medicine 42 (2012) 509–522

9. K.Somasundaram, et al. “Automated Skull Stripping Method using Clustering and Histogram Analysis for MRI Human Head Scans”, International Journal of Advanced Research in Computer Science & Technology, Vol. 2, Issue 3 (July - Sept. 2014)

10. K. Somasundaram, et al. “Fully automatic brain extraction algorithm for axial T2-weighted magnetic resonance images”, Computers in Biology and Medicine 40 (2010) 811–822

11. Sylvain Paris et al, “Bilateral Filtering: Theory and Applications”, Foundations and Trends in Computer Graphics and Vision, Vol. 4, No. 1 (2008) 1–73

12. Christian Lambert, et al. “Multiparametric brainstem segmentation using a modified multivariate mixture of Gaussians”, NeuroImage: Clinical, 684–694

13. Nigro S, Cerasa A, Zito G, Perrotta P, Chiaravalloti F, et al. (2014) Fully Automated Segmentation of the Pons and Midbrain Using Human T1 MR Brain Images. PLoS ONE 9(1): e85618. doi:10.1371/journal.pone.0085618

14. Chunming Li, Chenyang Xu, et al. “Distance Regularized Level Set Evolution and Its Application to Image Segmentation”, IEEE Transactions on Image Processing, Vol. 19, No. 12, 2010

15. Klein A, Ghosh SS, Avants B, Yeo B, Fischl B, Ardekani B, et al. “Evaluation of volume-based and surface-based brain image registration methods”. NeuroImage 2010; 51(1):214–20.

16. Wels M, Zheng Y, Huber M, Hornegger J, Comaniciu D. “A discriminative model-constrained EM approach to 3D MRI brain tissue classification and intensity non-uniformity correction”, Phys Med Biol 2011; 56(11): 3269–300.

17. Kolawole Oluwole Babalola et al. “An evaluation of four automatic methods of segmenting the subcortical structures in the brain”, NeuroImage 47 (2009) 1435–1447

18. Musicco M, “Gender differences in the occurrence of Alzheimer's disease”, Funct Neurol. 2009 Apr-Jun; 24(2):89-92.

19. K R Anandh, C M Sujatha , S Ramakrishnan , “Segmentation and Analysis of Corpus Callosum in Alzheimer MR Images using Total Variation Based Diffusion Filter and Level Set Method”, Biomedical sciences instrumentation, Apr 2015